valence–ionized Ne dimer is slow in comparison to ICD. The flatness of the inner-valence potential energy curves, which enables ICD at essentially all interatomic distances and prevents ultrafast dissociation, is specific to van der Waals systems. In real molecules such as O_2, electron-correlation effects are stronger: The adiabatic potential energy curves in the inner-valence regime are not flat and have many avoided crossings associated with steep dissociative curves. Real molecules can rapidly dissociate and convert electronic energy into kinetic energy of the dissociating fragments.

Finally, without triple-coincidence COLTRIMS experiments to locate the curve-crossing region and moment of onset of the Feshbach autoionizing state, accurate modeling of these superexcited states would not have been possible. Generally, electronic-structure methods, even for excited states, have made substantial progress. However, the inner-valence regime remains challenging because of the large number of electronic states involved and because of the considerable role that electronic many-body effects play in this highly excited energy regime.

We have uncovered the onset of an electronic Feshbach resonance and the existence of negative binding-energy states in neutral atoms. We show that it is possible to actively manipulate superexcited states above the ionization potential by interrupting autoionization with a strong femtosecond laser field. These findings should be applicable to autoionizing states in small molecules.

References and Notes

1. R. Santra, J. Zobeley, L. S. Cederbaum, N. Moiseyev, *Phys. Rev. Lett.* **85**, 4490 (2000).
2. T. Jahnke *et al*., *Phys. Rev. Lett.* **93**, 163401 (2004).
3. T. Jahnke *et al*., *J. Electron Spectrosc. Relat. Phenom.* **141**, 229 (2004).
4. R. Feifel, J. H. D. Eland, D. Edvardsson, *J. Chem. Phys.* **122**, 144308 (2005).
5. S. Hsieh, J. H. D. Eland, *J. Phys. At. Mol. Opt. Phys.* **29**, 5795 (1996).
6. S. D. Price, J. H. D. Eland, *J. Phys. At. Mol. Opt. Phys.* **24**, 4379 (1991).
7. L. Miaja-Avila *et al*., *Phys. Rev. Lett.* **101**, 046101 (2008).
8. M. Drescher *et al*., *Nature* **419**, 803 (2002).
9. B. Boudaiffa, P. Cloutier, D. Hunting, M. A. Huels, L. Sanche, *Science* **287**, 1658 (2000).
10. A. Kuleff, L. S. Cederbaum, *Phys. Rev. Lett.* **98**, 083201 (2007).
11. A. Rundquist *et al*., *Science* **280**, 1412 (1998).
12. E. Gagnon *et al*., *Science* **317**, 1374 (2007).
13. E. Gagnon *et al*., *Rev. Sci. Instrum.* **79**, 063102 (2008).
14. J. Yang *et al*., *J. Chem. Phys.* **128**, 091102 (2008).
15. A. Dreuw, L. S. Cederbaum, *Phys. Rev. A* **63**, 012501 (2000).
16. X.-B. Wang, L.-S. Wang, *Nature* **400**, 245 (1999).
17. H. Feshbach, *Ann. Phys.* **5**, 357 (1958).
18. C. A. Regal, C. Ticknor, J. L. Bohn, D. S. Jin, *Nature* **424**, 47 (2003).
19. S. Jochim *et al*., *Science* **302**, 2101 (2003).
20. L. S. Cederbaum *et al*., *J. Phys. B* **10**, L549 (1977).
21. M. Lundqvist, D. Edvardsson, P. Baltzer, M. Larsson, B. Wannberg, *J. Phys. At. Mol. Opt. Phys.* **29**, 499 (1996).
22. H. Lischka, R. Shepard, F. B. Brown, I. Shavitt, *Int. J. Quantum Chem. Symp.* **15**, 91 (1981).
23. R. Shepard *et al*., *Int. J. Quantum Chem. Symp.* **22**, 149 (1988).
24. H. Lischka *et al*., *Phys. Chem. Chem. Phys.* **3**, 664 (2001).
25. T. H. Dunning, *J. Chem. Phys.* **90**, 1007 (1989).
26. R. I. Hall, *et al*., *Phys. Rev. Lett.* **68**, 2751 (1992).
27. Y. Hikosaka, *et al*., *J. Chem. Phys.* **119**, 7693 (2003).
28. P. M. Dehmer, W. L. Luken, W. A. Chupka, *J. Chem. Phys.* **67**, 195 (1977).

29. We thank J. H. D. Eland and B. Krassig for helpful discussions. We acknowledge support for this work from NSF through the Physics Frontiers Centers Program and from the Office of Basic Energy Sciences, Office of Science, U.S. Department of Energy (DOE) (H.C.K. and M.M.M. under grant DOE DE-FG02-99ER14982; R.S. and P.H. under contract DE-AC02-06CH11357).

Supporting Online Material

www.sciencemag.org/cgi/content/full/322/5904/1081/DC1
SOM Text
Figs. S1 and S2
References

11 August 2008; accepted 15 October 2008
10.1126/science.1164498

Photosynthetic Control of Atmospheric Carbonyl Sulfide During the Growing Season

J. E. Campbell,[1]*† G. R. Carmichael,[2] T. Chai,[3] M. Mena-Carrasco,[4,5] Y. Tang,[2] D. R. Blake,[6] N. J. Blake,[6] S. A. Vay,[7] G. J. Collatz,[8] I. Baker,[9] J. A. Berry,[10] S. A. Montzka,[11] C. Sweeney,[12] J. L. Schnoor,[1] C. O. Stanier[2]

Climate models incorporate photosynthesis-climate feedbacks, yet we lack robust tools for large-scale assessments of these processes. Recent work suggests that carbonyl sulfide (COS), a trace gas consumed by plants, could provide a valuable constraint on photosynthesis. Here we analyze airborne observations of COS and carbon dioxide concentrations during the growing season over North America with a three-dimensional atmospheric transport model. We successfully modeled the persistent vertical drawdown of atmospheric COS using the quantitative relation between COS and photosynthesis that has been measured in plant chamber experiments. Furthermore, this drawdown is driven by plant uptake rather than other continental and oceanic fluxes in the model. These results provide quantitative evidence that COS gradients in the continental growing season may have broad use as a measurement-based photosynthesis tracer.

Parameterizations of carbon-climate feedbacks in climate models are based on climate sensitivities for photosynthesis and respiration that are highly uncertain (*1*–*3*). Measurement-based estimates of photosynthesis or respiration fluxes at large scales (>10^4 km^2) are needed to investigate these feedback mechanisms. Whereas photosynthesis and respiration-flux estimates have been made using eddy flux (*4*, *5*) and isotope techniques (*6*), robust tools for investigating these processes at large scales are currently lacking.

Recent work suggests potential for the use of atmospheric carbonyl sulfide (COS) as a photosynthesis tracer, on the basis of similarities observed between COS and CO_2 in a global air-monitoring network (*7*). The similarities are attributable to the simultaneous uptake of COS and CO_2 in photosynthetic gas exchange by terrestrial plants (*8*). COS has also been studied as a source of stratospheric aerosol (*9*, *10*), with recent reports suggesting that COS is a major source and that its contribution may be closely linked to continental surface fluxes (*11*, *12*).

Past models of COS plant uptake assume a 1:1 relation between relative uptake of COS and net primary productivity (NPP) (*13*–*16*). This relation was challenged by plant chamber (*8*) and atmospheric measurement studies (*7*), which suggest a new model of uptake that is related to photosynthesis [gross primary productivity (GPP)] and yields four to six times the uptake of the NPP-based models. COS uptake is related to GPP because atmospheric COS and CO_2 diffuse at similar rates into stomata, dissolve at similar rates into intercellular plant water, and are consumed by photosynthesis enzymes (*17*, *18*). COS is taken up preferentially to CO_2 because

[1]Department of Civil and Environmental Engineering, University of Iowa, Iowa City, IA 52242, USA. [2]Center for Global and Regional Environmental Research, University of Iowa, Iowa City, IA 52242, USA. [3]Science and Technology Corporation, Hampton, VA 23666, USA. [4]Department of Environmental Engineering, Universidad Andrés Bello, Santiago, Chile. [5]Molina Center for Energy and the Environment, Massachusetts Institute of Technology, Cambridge, MA 02139, USA. [6]Department of Chemistry, University of California, Irvine, CA 92697, USA. [7]NASA Langley Research Center, Hampton, VA 23681, USA. [8]Biospheric Sciences Branch, NASA-Goddard Space Flight Center, Greenbelt, MD 20771, USA. [9]Department of Atmospheric Science, Colorado State University, Fort Collins, CO 80523, USA. [10]Department of Global Ecology, Carnegie Institution of Washington, Stanford, CA 94305, USA. [11]Global Monitoring Division, National Oceanic and Atmospheric Administration (NOAA) Earth System Research Laboratory, Boulder, CO 80305, USA. [12]Cooperative Institute for Research in Environmental Sciences, University of Colorado, Boulder, CO 80304, USA.

*Present address: College of Engineering, University of California, Merced, CA 95344, USA.
†To whom correspondence should be addressed. E-mail: ecampbell3@ucmerced.edu

photosynthesis enzymes transform one-third of the dissolved CO_2 in leaf water but irreversibly transform most of the dissolved COS (*19*, *20*). The remainder of the dissolved CO_2 diffuses back to the atmosphere. The chamber studies suggest a GPP-based uptake model

$$F = GPP \cdot \frac{[COS]}{[CO_2]} \cdot V_{COS/CO_2} \qquad (1)$$

where F is COS plant uptake, GPP is the photosynthetic uptake of CO_2 by terrestrial plants, $[COS]/[CO_2]$ is the ratio of ambient concentrations, and V_{COS/CO_2} is the leaf-scale relative uptake measured during plant chamber experiments.

This GPP-based model was found in recent work to be qualitatively consistent with variations of global atmospheric measurements, suggesting that the total atmospheric lifetime of COS is only 1.5 to 3 years (*7*, *21*). However, it remains to be determined whether atmospheric COS measurements are quantitatively consistent with GPP-based plant uptake.

To provide a quantitative test of the relation between GPP and atmospheric COS, we compared atmospheric COS measurements from an airborne experiment with two simulations from a three-dimensional atmospheric transport model; one simulation was driven by the GPP-based uptake, and the second was driven by the NPP-based uptake. The airborne experiment, the Intercontinental Chemical Transport Experiment–North America (INTEX-NA), included 1741 daytime measurements of COS over continental North America between the surface and 12 km in altitude during July and August 2004. The experiment also included measurements of CO_2 (*22*) and many other species (*23*). We compared these INTEX-NA observations to the NOAA Earth System Research Laboratory (NOAA/ESRL) airborne observations made during July and August of 2005, 2006, and 2007 (*7*). To interpret the INTEX-NA observations, we simulated COS and CO_2 concentrations over North America for the INTEX-NA period (*24*, *25*). The COS simulations were driven by plant uptake, soil sinks, and ocean and anthropogenic sources (direct and indirect). We calculated GPP-based plant uptake (Eq. 1) by scaling regional GPP fluxes (*26*) by leaf-scale relative uptake estimates. The NPP-based uptake and other surface fluxes were taken from a recent inventory of gridded surface fluxes (*14*). We simulated CO_2 concentrations using ecosystem, ocean, and anthropogenic surface fluxes. See the supporting online material (SOM) for details on observations and model simulations.

The persistent vertical drawdown (Fig. 1) and variability (Fig. 2) in the boundary layer are well represented by the GPP model, whereas the NPP model performs poorly. Plant uptake was found to be dominant over other sources and sinks in the continental COS budget during the growing season (Fig. 3), a necessary condition for the use of COS as a photosynthesis tracer. These results are discussed below.

The mean modeled and measured CO_2 concentrations along the INTEX-NA flight paths (Fig. 1A) show the expected net uptake of CO_2 and boundary-layer mixing during the growing season (*27*). The agreement between the observed and modeled drawdown indicates that atmospheric mixing is well represented in the model. Whereas model underestimation in the 2- to 5-km altitude range may suggest some deficiencies in the simulated mixing, there is only a 10% difference between the observed and modeled estimates of the column-integrated drawdown (*21*).

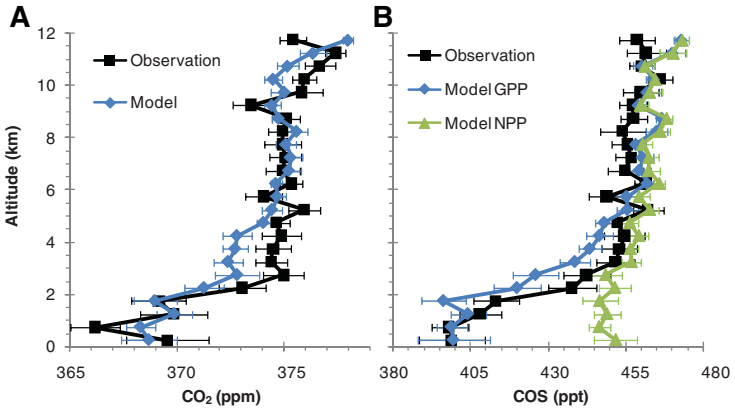

Fig. 1. Vertical profiles of COS and CO_2 along INTEX-NA flight paths. Mean concentrations for all continental INTEX-NA data for CO_2 (**A**) and COS (**B**) (error bars indicate ± 95% CI, n = 70 average observations in each bin). Model results were interpolated to time and location of each observation. ppm, parts per million.

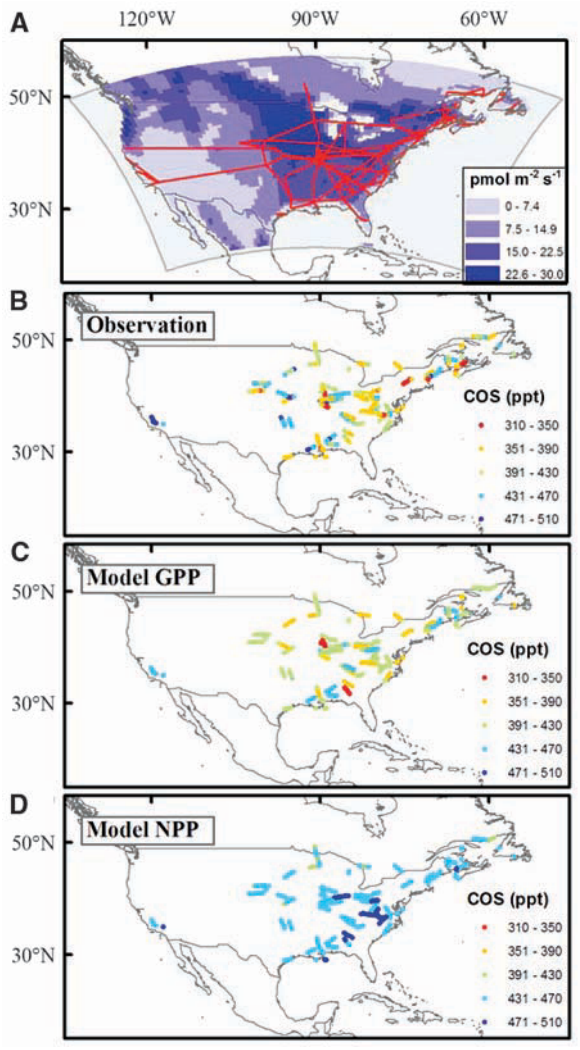

Fig. 2. COS plant uptake flux and boundary-layer concentrations. (**A**) COS plant uptake flux (mean July 2004) calculated by scaling modeled GPP by leaf-relative uptake. See SOM for details. Continental INTEX-NA DC8 flight paths (red lines) are shown within the model domain (gray box). (**B** to **D**) Modeled and observed atmospheric COS concentrations at all continental sampling points under 2 km in altitude above sea level (ASL).

The mean COS vertical profile (from the 1741 INTEX-NA samples) also shows considerable drawdown in the boundary layer (Fig. 1B). The INTEX-NA concentration drawdown (difference between 6 to 8 km and 0 to 2 km in altitude) of 59.9 ± 8.9 parts per thousand (ppt) [mean ± 95% confidence interval (CI), n = 50 vertical profiles] for sampling in July and August of 2004 is consistent with the NOAA/ESRL drawdown of 55.9 ± 19.0 ppt (mean ± 95% CI, n = 12 airborne sites) for sampling in July and August of 2005 through 2007. The NPP model largely underestimates the observed drawdown as expected (*13*, *16*), whereas the GPP model has good agreement with the observed drawdown. As with CO_2, some deficiencies in the GPP model are apparent in the 2- to 5-km altitude range. However, there is only a 15% difference between the observed and GPP model estimates of the column-integrated drawdown (*21*). The column-integrated drawdown for the observed data was 4.2 times the NPP model estimate (*21*). Sensitivity analysis showed that the drawdown estimates are robust with respect to boundary condition uncertainty (*21*).

Maps of INTEX-NA boundary-layer COS concentrations show considerable variability in the boundary-layer observations (SD = 39 ppt), and this variability is similar to that in the GPP model (SD = 34 ppt) but much larger than that in the NPP model (SD = 24 ppt) (Fig. 2). The GPP model captures much of the observed variability in the boundary-layer COS concentrations with a correlation coefficient of 0.71 (n = 440). This GPP model performance is similar to the a priori performance in CO_2 studies that use a model-observations analysis to infer surface-flux estimates (*28*). The variability in the GPP model is largely driven by the magnitude of the plant uptake and caused by the mixing of background air with boundary-layer air that is depleted of COS (*21*).

The combined evidence from the concentration drawdown, column-integrated drawdown, boundary-layer variation, CO_2 profiles, and NOAA/ESRL data are consistent with the GPP-based model rather than the NPP-based model. Next, we consider the relative influence of the different surface fluxes on the COS airborne samples using transport simulations driven by only one surface flux at a time (Fig. 3A). Anthropogenic COS emissions (direct and indirect) are concentrated in the eastern United States but result in a boundary-layer enhancement that is less than one-third of the vegetative drawdown (*21*). The COS soil up-

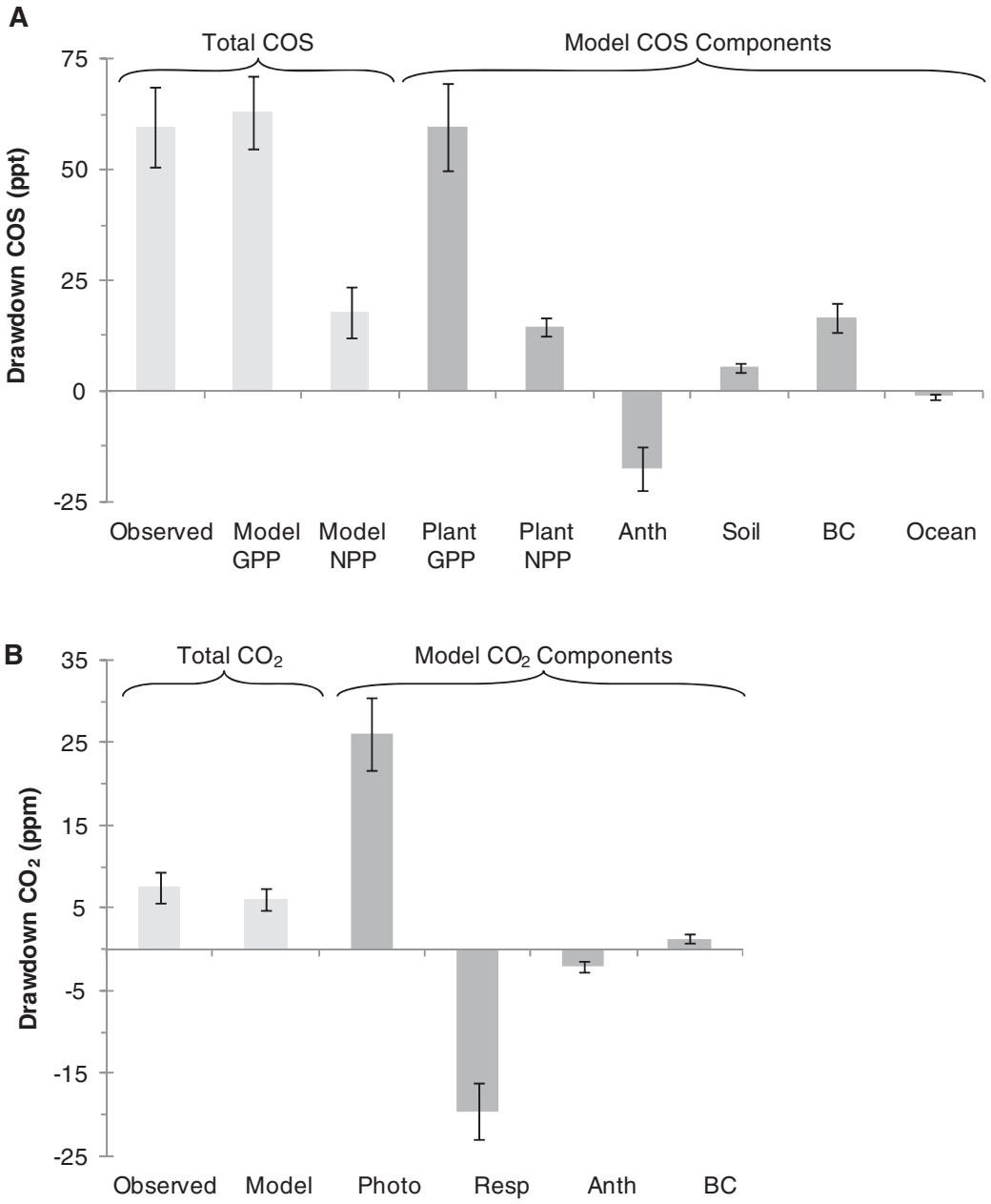

Fig. 3. Tropospheric drawdown for observed and modeled concentrations along continental INTEX-NA flight paths. Tropospheric drawdown of COS (**A**) and CO_2 (**B**), for total (left bracket) and modeled components (right bracket) as the difference between mean 6- to 8-km and 0- to 2-km altitude ASL concentrations for all continental INTEX-NA data (error bars indicate ± 95% CI, n = 50 vertical profiles). Anth, anthropogenic; Photo, photosynthesis; Resp, ecosystem respiration; BC, boundary condition. Positive drawdown is removal from the atmosphere, and negative drawdown is a source to the atmosphere. Individual component drawdowns (right bracket) are based on multiple atmospheric transport model simulations using only one flux at a time as input and fixed boundary conditions.

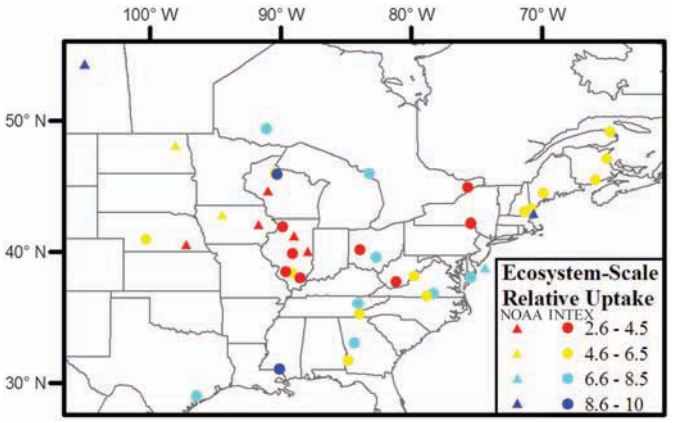

Fig. 4. Observed ERU of COS to CO_2 from INTEX-NA and NOAA/ESRL measurements. ERU is the normalized drawdown of COS relative to the normalized drawdown of CO_2, calculated from the difference between airborne observations in the 0- to 2-km and 6- to 8-km altitude bins. Samples were taken in July and August 2004 for INTEX-NA (circles) and July and August of 2005 through 2007 for NOAA/ESRL (triangles). Repeated vertical profiles at the same location are shown as a single average. (See SOM for details.)

take is <10% of the plant uptake, which is consistent with available field observations (*29*). Although ocean fluxes are a large source globally (*14*), they have only a small influence on the vertical profile for the continental growing season. There may be large missing sources in the global COS budget that could be important in relation to plant uptake for some regions (*8*). However, the good agreement of modeled and observed COS during INTEX-NA suggests that these missing sources are not located in North America during the growing season. Whereas the COS drawdown is dominated by plant uptake, the CO_2 drawdown has offsetting influences of photosynthesis and respiration components that are many times the net CO_2 drawdown (Fig. 3B). These offsetting components make it challenging to apply CO_2 measurements to separately investigate photosynthesis and respiration, reinforcing the need for a tracer such as COS.

This evidence that continental-scale variations of atmospheric COS over North America are driven by the COS/photosynthesis relation suggests the potential use of COS as a carbon-cycle tracer. One tracer application is to estimate the ratio of GPP CO_2 fluxes relative to net ecosystem exchange (NEE) CO_2 fluxes using relations between simultaneous observations of COS and CO_2. For vertical profile observations, a useful relation is the ecosystem-scale relative uptake (ERU), which is the ratio of the relative drawdown of COS to CO_2 (*7*, *21*). When plant uptake is the dominant flux, the ERU is proportional to the ratio of GPP/NEE with a proportionality constant that is the leaf-scale relative uptake. The INTEX-NA and NOAA/ESRL observations have a mean ERU of 5.7 ± 0.6 (mean ± SD, $n = 31$ vertical profiles, July and August 2004) and 5.7 ± 2.1 (mean ± SD, $n = 10$ airborne sites, July and August of 2005 through 2007), respectively. For a mean continental leaf-scale relative uptake of 2.2 (*21*), these ERU values imply a GPP/NEE ratio of 2.6, which is similar to estimates of GPP/NEE of crops during mid–growing season from eddy-flux studies (*5*, *7*, *30*). Both INTEX-NA and NOAA/ESRL observations show lower ERU values over the mid-continent where C4 corn is extensive (Fig. 4). This regional depression in ERU could reflect a decrease in the ratio of GPP/NEE for C4 corn plants that has also been observed in eddy covariance studies of the North American growing season (*5*). Alternatively, lower leaf-scale relative uptake values have been hypothesized for C4 plants (*7*, *8*) and we suggest that the leaf-scale relative uptake and the ratio of GPP/NEE for C4 plants be explored more widely. Although the ERU could also be influenced by a regional anthropogenic COS source, the anthropogenic source relative to the plant uptake is rather weak in this region (*21*).

Another tracer application is to estimate the photosynthesis CO_2 flux with the use of an inverse analysis (*31*) of the COS model concentration error. Inverse analyses must consider multiple sources of model error, including transport parameterizations, different surface fluxes, boundary conditions, and representation error. For the COS inversion, the two flux parameters, other than GPP (Eq. 1), must be well constrained, and the COS fluxes other than plant uptake must be well known or relatively small, as may be the case for the continental growing season. One flux parameter, the concentration ratio parameter (Eq. 1), is well constrained by observations and has an observed variability of <10% in the INTEX-NA boundary-layer samples ($n = 440$). The other flux parameter, leaf-scale relative uptake, may be more uncertain because of the dependence on plant type and growth conditions, but the success of the simple leaf-scale uptake mapping used in this work is promising (*21*). Knowledge of leaf-scale uptake could be improved with additional plant chamber and ambient studies in support of efforts to recover GPP values.

The results presented here suggest global COS plant uptake and vertical gradients that are more than four times those predicted in previous global models (*14*–*16*). This finding implies a large missing source in the global COS budget (*7*, *8*) and large uncertainty in how previous global models have predicted the transfer of COS to the stratosphere. Applications of the GPP model at a global scale should help to resolve uncertainties in COS budgets and could improve our understanding of the relation between COS surface fluxes and stratospheric aerosol. However, the most intriguing application may be to recover GPP and ecosystem respiration information by inverse analysis of atmospheric COS measurements.

References and Notes

1. P. M. Cox, R. A. Betts, C. D. Jones, S. A. Spall, I. J. Totterdell, *Nature* **408**, 184 (2000).
2. C. B. Field, D. B. Lobell, H. A. Peters, N. R. Chiariello, *Annu. Rev. Environ. Resour.* **32**, 1 (2007).
3. P. Friedlingstein *et al.*, *J. Clim.* **19**, 3337 (2006).
4. P. Ciais *et al.*, *Nature* **437**, 529 (2005).
5. E. Falge *et al.*, *Agric. For. Meteorol.* **113**, 53 (2002).
6. D. R. Bowling, P. P. Tans, R. K. Monson, *Global Change Biol.* **7**, 127 (2001).
7. S. A. Montzka *et al.*, *J. Geophys. Res.* **112**, D09302 (2007).
8. L. Sandoval-Soto *et al.*, *Biogeosciences* **2**, 125 (2005).
9. M. Chin, D. D. Davis, *J. Geophys. Res.* **100**, 8993 (1995).
10. P. J. Crutzen, *Geophys. Res. Lett.* **3**, 73 (1976).
11. J. Notholt *et al.*, in *SPARC Assessment of Stratospheric Aerosol Properties (ASAP)*, L. Thomason, T. Peter, Eds. (World Meteorological Organization World Climate Research Programme, Toronto, 2006), pp. 29–76.
12. J. Notholt *et al.*, *Science* **300**, 307 (2003).
13. N. J. Blake *et al.*, *J. Geophys. Res.* **113**, D09S90 (2008).
14. A. J. Kettle, U. Kuhn, M. von Hobe, J. Kesselmeier, M. O. Andreae, *J. Geophys. Res.* **107**, 4658 (2002).
15. A. J. Kettle *et al.*, *Atmos. Chem. Phys.* **2**, 343 (2002).
16. E. Kjellström, *J. Atmos. Chem.* **29**, 151 (1998).
17. G. Protoschill-Krebs, J. Kesselmeier, *Bot. Acta* **105**, 206 (1992).
18. G. Protoschill-Krebs, C. Wilhelm, J. Kesselmeier, *Atmos. Environ.* **30**, 3151 (1996).
19. G. D. Farquhar *et al.*, *Nature* **363**, 439 (1993).
20. R. J. Francey, P. P. Tans, *Nature* **327**, 495 (1987).
21. Materials and methods are available as supporting material on *Science* Online.
22. Y. H. Choi *et al.*, *J. Geophys. Res.* **113**, D07301 (2008).
23. H. B. Singh, W. H. Brune, J. H. Crawford, D. J. Jacob, P. B. Russell, *J. Geophys. Res.* **111**, D24S01 (2006).
24. J. E. Campbell *et al.*, *Tellus B* **59B**, 199 (2007).
25. G. R. Carmichael *et al.*, *J. Geophys. Res.* **108**, 8823 (2003).
26. S. C. Olsen, J. T. Randerson, *J. Geophys. Res.* **109**, D02301 (2004).
27. C. Gerbig *et al.*, *J. Geophys. Res.* **108**, 4757 (2003).
28. D. M. Matross *et al.*, *Tellus B Chem. Phys. Meterol.* **58**, 344 (2006).
29. M. Steinbacher, H. G. Bingemer, U. Schmidt, *Atmos. Environ.* **38**, 6043 (2004).
30. A. E. Suyker, S. B. Verma, G. G. Burba, T. J. Arkebauer, *Agric. For. Meteorol.* **131**, 180 (2005).
31. C. D. Rodgers, *Inverse Methods for Atmospheric Sounding: Theory and Practice* (World Scientific, Singapore, 2000), p. 238.

32. We thank J. Kettle for COS flux data and C. Tebaldi, J. Dungan, T. Campbell, and D. Campbell for critical comments on the manuscript. This research was supported by a NASA Earth System Science Graduate Fellowship, Center for Global and Regional Environmental Research, NOAA Office of Oceanic and Atmospheric Research contribution to the North American Carbon Program, NASA INTEX, and NSF Information Technology Research grants. NOAA observations of COS and CO_2 were made possible by the assistance of P. Tans, C. Sweeney, L. Miller, T. Conway, P. Lang, C. Siso, and B. Hall.

Supporting Online Material

www.sciencemag.org/cgi/content/full/322/5904/1085/DC1
Materials and Methods
SOM Text
Figs. S1 to S5
Tables S1 to S3
References

31 July 2008; accepted 17 October 2008
10.1126/science.1164015